# MINFLUX nanoscopy to study the NK cell immune synapse

**Nora Ross[a,1], Daniel P. Leaman[b], Jessica Matthias[c], Michael B. Zwick[b], Emily M. Mace[d], Scott C. Henderson[e,f], and Charles Daniel Murin[a,e,*]**

[a]San Diego Biomedical Research Institute, San Diego, CA, USA
[b]Department of Immunology and Microbiology, Scripps Research, La Jolla, CA, USA
[c]Abberior Instruments America, Bethesda, MD, USA
[d]Department of Pediatrics, Columbia University Irving Medical Center, New York, NY, USA
[e]Department of Integrative Structural and Computational Biology, Scripps Research, La Jolla, CA, USA
[f]Core Microscopy Facility, Scripps Research, La Jolla, CA, USA
*Corresponding author. e-mail address: dmurin@sdbri.org

## Contents

1. Introduction 2
2. Materials 4
   2.1 Disposables 4
   2.2 Common equipment 4
   2.3 Specialized equipment 5
   2.4 Reagents 5
   2.5 Cell culture 7
3. Methods 7
   3.1 Cell maintenance 7
   3.2 Cell line generation 8
   3.3 Liposome formation 9
   3.4 SLB preparation 10
   3.5 Synapse formation 12
   3.6 Sample labeling for MINFLUX imaging 12
   3.7 Sample mounting for MINFLUX imaging 13
   3.8 MINFLUX data acquisition 13
   3.9 MINFLUX data processing 16
4. Limitations 20
5. Concluding remarks 20
6. Notes 21
Acknowledgments 23
Declaration of interests 23
References 23

[1] Currently at the Department of Applied Physics, Science for Life Laboratory, KTH Royal Institute of Technology, Stockholm, Sweden

*Methods in Cell Biology*
ISSN 0091-679X, https://doi.org/10.1016/bs.mcb.2026.01.021

## Abstract

Antibody dependent cellular cytotoxicity (ADCC) is an effector function performed by natural killer (NK) cells to target and clear viral infections and cancer. ADCC is a critical feature of several antibody and cellular therapeutics as well as vaccination strategies. Using microscopy to understand the details of molecular events driving ADCC is essential to improving such therapeutics but has been limited by technologies that cannot practically provide the spatial resolution necessary to study protein function at the single molecule level in cells. In this chapter, we describe a model system using MINFLUX nanoscopy to study the molecular distribution of human FcγRIIIa (CD16a), the IgG receptor, in the NK cell immunological synapse during ADCC. The technique described here will enable further exploration of how CD16a drives NK cell ADCC and can also be applied to the study of other important protein receptors for which nanometer localization precision is needed.

## 1. Introduction

Antibody mediated effector functions are a critical component of the humoral immune system that are important for the clearance of foreign pathogens and virally infected cells. Antibody effector functions are therefore of clinical importance to the development of therapeutic monoclonal antibodies for the treatment of cancer and infectious disease as well as for vaccination strategies. Natural killer (NK) cells are a subset of innate immune lymphocytes capable of performing antibody dependent cellular cytotoxicity (ADCC) through the interaction of the Fc domain of an IgG with FcγRIIIa (CD16a) (Lanier et al., 1986, 1988). NK cells perform their cytolytic function through the formation of a tight cell-cell contact referred to as the immunological synapse (IS) (Mace et al., 2014; Orange, 2008).

Our understanding of the NK cell IS has benefited from both technical advancements in light microscopy and new model systems that together facilitate studying different aspects of the IS (Mukherjee et al., 2017; Zheng et al., 2015a; Mace & Orange, 2013a). The application of imaging techniques such as lattice light-sheet and stimulated emission depletion (STED) nanoscopy unlocked the ability to describe dynamics of the immune synapse such as actin remodeling and details around NK cell degranulation (Hazime et al., 2025; Mace & Orange, 2014; Mace et al., 2012; Rak et al., 2011). Furthermore, stochastic optical reconstruction microscopy (STORM) opened the possibility to describe receptor distribution and clustering (Ambrose et al., 2020; Bláha et al., 2022; Rossy et al., 2013; Sajman et al., 2021).

However, with a practical localization precision in the tens of nanometers, none of these super-resolution techniques can provide the resolution necessary to describe protein oligomerization and complex interactions. Since we sought to determine the molecular arrangement of CD16a, we calculated that we would need spatial precision on the single nanometer scale. The development of MINFLUX nanoscopy, which utilizes the zero intensity of a doughnut shaped excitation beam to gradually approach the position of a fluorophore, enables the description of fluorophore positions with better than 3 nm localization precision, opening the possibility to measure distances between individual proteins or track protein dynamics inside the IS with increased spatial precision and temporal resolution than other super-resolution techniques. Therefore, MINFLUX is ideally suited to answer the questions we proposed on a biological scale with true single molecule precision and within a cellular environment.

A question facing our current understanding of NK cell ADCC is: how does CD16a spatially distribute in the NK cell membrane at the IS during activation? Here, we provide a model of the NK cell IS to study the spatial distribution of CD16a at the single molecule level. We developed a supported lipid bilayer (SLB) that includes both HER2, a target of therapeutic monoclonal antibodies, and ICAM-1, which is important for both NK cell adhesion and CD16a signaling (Steblyanko et al., 2015). We then harnessed the application of MINFLUX nanoscopy to determine high precision localizations of CD16a within the cellular environment (Balzarotti et al., 2017; Gwosch et al., 2020; Schmidt et al., 2021). With this method, we show that CD16a clustering increases during ADCC, and we identified pairs of fluorophores conjugated to SNAP tagged CD16a separated by ~18 nm that form the basal signaling unit (Ross et al., 2025). Using molecular dynamics and artificial intelligence-based modeling, we show biophysically valid structures indicating that these CD16a pairs could be homodimers, an oligomeric arrangement that may be relevant to their biological function. Therefore, our methodology forms a foundation to further study CD16a in the NK cell membrane to improve our understanding of ADCC, providing new paradigms to aid the development of improved therapeutics and vaccination strategies. This technique should be widely applicable to other aspects of NK cell immune signaling biology and has relevance to a diverse set of signaling molecules in cells like B-cell, T-cells and other cytolytic immune cells.

# 2. Materials

## 2.1 Disposables

1. 1.5 mL microcentrifuge tubes (0030123611, Eppendorf)
2. 15 mL centrifuge tube (89039-666, VWR)
3. 50 mL centrifuge tube (89039-656, VWR)
4. Disposable glass culture tubes (14-961-28, Fisher Scientific)
5. 4 mL screw top glass vials (111009391, Millipore Sigma)
6. Cell culture flasks 25 $cm^2$ (Nunc™ 169900, ThermoFisher)
7. #1.5H glass coverslip, 25 mm × 75 mm (10812, Ibidi)
8. Sticky-Slide VI 0.4 (80608, Ibidi)
9. Nunc™ 96-well polystyrene round bottom microwell plates (268200, Thermo Fisher)
10. Nunc™ 6- and 12-well, non-treated multidish (150239, 150200, Thermo Fisher)
11. Glass Pasteur pipettes (14672-380, VWR)
12. Pipette tips 10, 200 and 1000 μL, non-filter (2042. S, 2102. S, 2372. S, Neptune)
13. Pipette tips 10, 200 and 1000 μL, filter (BT10, BT200, BT1000.96, Neptune)
14. Serological pipettes, sterile, individually wrapped 5, 10, 25 mL (76201-710, 75816-100, 75816-090, VWR)
15. Kimtech Science™ Kimwipes™ Delicate Task Wipes, 2 Ply (34705, Kimberly-Clark)
16. Nalgene™ Rapid-Flow™ sterile disposable filter unit with PES (09-741-02, Fisher Scientific)
17. PC membranes, 0.8, 0.4, 0.2 and 0.1 μm (610009, 610007, 610006, 610005, Avanti)
18. Whatman filter discs (610014, Avanti)

## 2.2 Common equipment

1. Cell culture incubator allowing standing cell culture conditions in a humidified atmosphere (37°C, 5 % $CO_2$) and cell culture laminar flow hood (BSL-2)
2. Chemical hood for cell fixation and staining
3. Sorvall Legend Micro17R. refrigerated microcentrifuge (75002440, Thermo Scientific)
4. Vortex mixer (S0200, Labnet International)
5. Cell counter (6749, Corning)

6. Water bath set at 37°C
7. Platform shaker
8. Thermo Scientific MaxQ 8000 Incubator Shaker

## 2.3 Specialized equipment

9. Medi-Vac® Guardian™ Canister 2000 mL Shut-off valve/locking lid (65651-200, Medex Supply), outfitted with a filter and tubing to vacuum source
10. Swing bucket centrifuge capable of holding 15 and 50 mL micro-centrifuge tubes (Thermo Fisher)
11. PELCO easiGlow™ Glow Discharge Cleaning System outfitted with a vacuum pump (92100S and 92083, Ted Pella, Inc.)
12. Branson Ultrasonics™ CPXH Series Ultrasonic Cleaning Bath (13-336-120, Fisher Scientific)
13. 1 mL Hamilton syringes (1001, Hamilton)
14. Mini extruder set with holder/heating block (610000, Avanti)
15. Bel-Art Space Saver vacuum desiccator, 0.2 cu. ft (F42022-0000, Bel-Art)
16. Lonza 4D-Nucleofector® X Unit (AAF-1003X, Lonza)
17. Mr. Frosty™ Freezing Container (5100-0001, Thermo Fisher)
18. BRAND® glass staining trough with lid (BR472200-10EA, Millipore Sigma)
19. Proline® Plus adjustable-volume mechanical pipettes, 0.3-3 μL, 2-20 μL, 20-200 μL, 100-1000 μL (728010, 728030, 728060, 728070, Sartorius)
20. S1 Pipete fillers (9501, Thermo Fisher)
21. MoFlo Astrios EQ jet-in-air sorting flow cytometer (Beckman Coulter)
22. Zeiss LSM 880 Airyscan laser scanning confocal microscope, equipped with perfect focus and operated with Zen software 2.3 SP1 FP3 (Black).
23. MINFLUX 3D microscope equipped with an Olympus UPlanXApo 100x/1.40 Oil 8/0.17/FN26.5 objective lens, a 640 nm continuous-wave (CW) 80 mW laser and a 488 nm pulsed 1 mW laser for excitation, and a 405 nm CW 50 mW laser for activation. The system is controlled via Imspector software (version 16.3.15645-m2205) with MINFLUX drivers (Abberior Instruments).

## 2.4 Reagents

1. PBase Plasmid, such as pRP[Exp]-mCherry-CAG > hyPBase (VB010000-9365tax, VectorBuilder)

2. Plasmid carrying gene of interest compatible with PiggyBac system, such as pPB[Exp]-EF1A > EGFP/Neo (VB010000-9491dkf, VectorBuilder)
3. P1 Primary Cell 4D-Nucleofector® X Kit L (V4XP-1012, Lonza)
4. Alexa Fluor® 647 anti-human CD16 antibody (302023, Biolegend)
5. Alexa Fluor™ 488 Biosimilar Anti-Human HER2 (570381, BD Pharmingen)
6. Human HER2/ErbB2 Protein, His tag (HE2-H5225-100ug, Acros Biosystems)
7. Human ICAM-1/CD54 Protein, His tag (IC1-H52H5-100ug, Acros Biosystems)
8. Acetone (A18P-4, Fisher Scientific)
9. Ethanol (BP28184, Fisher Scientific)
10. Isopropanol (383910025, Thermo Fisher)
11. 1-palmitoyl-2-oleoyl-glycero-3-phosphocholine, POPC, in chloroform (850457C-25mg, Avanti)
12. 1,2-dioleoyl-sn-glycero-3-[(N-(5-amino-1-carboxypentyl)iminodiacetic acid)succinyl] (nickel salt), 18:1 DGS-NTA(Ni), in chloroform (790404C-5mg, Avanti)
13. Drierite (AC219090020, Fisher Scientific)
14. Ultrapure water (filtered using Millipore Milli-Q® purification system)
15. 10X PBS, pH 7.4 (IB70165, IBI Scientific)
16. $NiCl_2$ (339350-50 G, Millipore Sigma)
17. Trastuzumab, anti-HER2 (A2007, Selleckchem)
18. Paraformaldehyde (150146, MP Biomedicals)
19. Dimethyl sulfoxide (D8418, Sigma Aldrich)
20. Triton™ X-100 (T8787, Millipore Sigma)
21. $NH_4Cl$ (213330, Millipore Sigma)
22. Bovine serum albumin (10735078001, Millipore Sigma)
23. Antibiotic-Antimycotic, 100X (15240062, Gibco)
24. Image-iT™ (R37814, Thermofisher)
25. Dithiothreitol (P2325, Thermofisher)
26. SNAP-Surface® Alexa Fluor® 647 (S9136S, New England Biolabs)
27. Flash Phalloidin™ Green 488 (424201, Biolegend)
28. Gold 1% on titanium dioxide extrudates (150 nm diameter), AUROlite Au/$TiO_2$ (79-0165, Strem)
29. GLOX buffer, pH 8.0, mixed fresh
    a. 50 mM Tris-HCl (T3253-100G, Millipore Sigma)
    b. 10 mM NaCl (S9625-500G, Millipore Sigma)
    c. 10 % (w/v) glucose (G5767-25G, Millipore Sigma)

**d.** 10 mM MEA, cysteamine hydrochloride (M6500, Sigma-Aldrich; stock 1 M in 0.25 N HCl, store at 4 C for one week)
**e.** 40 μg/mL bovine-liver catalase (C100-50mg, Sigma-Aldrich)
**f.** 100 μg/mL glucose oxidase from *Aspergullus niger*, type VII (G2133, Sigma-Aldrich; stock 70 mg/mL in 50 mM Tris-HCl, made fresh)

**30.** Parafilm
**31.** Nitrogen gas source with regulator
**32.** Immersion oil (for FRAP studies: Immersol 518, Zeiss, Immersol W 210, Zeiss, for MINFLUX: Immil-F30CC, Olympus)

### 2.5 Cell culture

**1.** NK-92 cells (CRL-2407, ATCC)
**2.** Myleocult™ H5100 (05150, Stemcell Tech)
**3.** Human IL-2 recombinant protein, PeproTech® (200-02-50ug, Thermo Fisher)
**4.** Gibco™ Fetal Bovine Serum, heat inactivated (A5256801, Thermo Fisher)
**5.** Gibco™ RPMI 1650 Medium (11875093, Thermo Fisher)

## 3. Methods

### 3.1 Cell maintenance

This protocol utilizes the NK-92 cell line, an immortalized NK cell line commonly used to study NK cell function. NK-92 cells have been used as a cell therapy to treat several different types of cancer (Klingemann et al., 2016). This section outlines how parent and NK-92 cell lines were maintained after cryo-preservation.

**1.** Remove a vial of 1 mL NK-92 cells from liquid nitrogen and place on dry ice (typically 1 $\times 10^7$ cells total). Cells are typically stored in 10 % (v/v) DMSO/90 % (v/) FBS.
**2.** Prepare complete Myleocult medium. Myleocult, FBS, and Antibiotic-Antimycotic are stored at −20°C, so will first need to be thawed in a 37°C water bath. Add 56 mL of FBS and 5.6 mL of Antibiotic-Antimycotic to 500 mL of Myleocult. Filter through a 0.2 μm filter unit and store at 4°C when not being used (can be stored for up to 3 months).
**3.** Place vial in a bath of water at 37°C and swirl gently until a small amount of ice remains in the vial.
**4.** Sterilize the vial thoroughly with 70 % ethanol and place in a biosafety cabinet.

5. Gently pipette cells into a 15 mL centrifuge tube containing 9 mL of pre-warmed complete Myleocult medium.
6. Centrifuge cells at 300 × g for 5 min at room temperature.
7. Aspirate media with a sterile glass Pasteur pipette into a medivac suction canister. Resuspend the cell pellet gently with 10 mL of pre-warmed complete Myleocult medium. Add 200 IU/μL of IL-2 to the media. Cells can also be seeded at $4 \times 10^5$/mL, though we tend to seed at a higher density when first thawing cells.
8. Add resuspended cells to a T25 flask and place standing vertically in a cell culture incubator (37 °C, 5 % $CO_2$).
9. When first thawing cells, passage cells every 3 – 4 days by removing cells and centrifuging at 300 × g for 5 min (*see* **Note 1**).
10. Aspirate old medium and gently resuspend cells in about 1 mL of in fresh medium. Count cells using a cell counter.
11. Dilute cells at $4 \times 10^5$ cells/mL with fresh media and transfer to a T25 flask for culture. Add fresh IL-2 at 200 IU/μL each time cells are passaged.
12. After 2-3 passages, cells can be split 1:5 in fresh media with IL-2 at 100-200 IU/μL (*see* **Notes 2** and **3**).

## 3.2 Cell line generation

To facilitate localization of CD16a in NK cells, NK-92 cells were engineered to express SNAP-tagged CD16a (on the C-terminus). NK-92 cells do not endogenously express CD16a, therefore only the CD16a introduced through genetic engineering will be visualized. In this section we provide details on how the NK-$92^{CD16a\text{-}SNAP}$ cell line was generated through electroporation utilizing the piggyBac transposase.

1. Gently resuspend and count cells (*see* **Note 4)**, then transfer $3 \times 10^6$ cells to a 15 mL tube, and centrifuge at 100 × g for 10 min.
2. Meanwhile, add 500 μL of complete Myleocult medium to a 12 well plate and place in the incubator to stay warm and equilibrate pH. Then prepare a mixture of Nucleofector Solution and Supplement (following instructions provided by the Lonza Kit) and mix with 3 μg of target gene plasmid and 1 μg of PBase plasmid (*see* **Note 5**).
3. Remove medium from 15 mL tube and re-suspend cells in 100 μL of Lonza transfection solution containing plasmids, then transferred to the included cuvette from Lonza. (*see* **Note 6**)

4. Transfer the cuvette to the electroporation device and nucleofect using program CA-137.
5. When the program is complete, add 500 μL of warm, complete Myleocult medium to the cuvette and transfer the contents of the cuvette to the pre-warmed 12 well plate and place the plate back in the cell culture incubator.
6. Maintain the cells for 1 week, exchanging the media every 2 – 3 days before isolating CD16a positive cells by flow assisted cell sorting (FACS) (*see* **Note 7** and **8**).
7. Allow the sorted cells to recover for 3 – 4 days in a round-bottom, 96-well plate containing 200 μL of complete Myleocult medium (adding 200 IU/μL IL-2) and then begin to expand them. Once cells are sufficiently expanded, make stocks with at least $3 \times 10^6$ cells per vial in 10 % (v/v) DMSO and 90 % (v/v) FBS. Slowly freeze cell stocks in a Mr. Frosty at −80°C overnight, then store long-term above liquid nitrogen. The cells prepared through this protocol are referred to at NK-92$^{CD16a\text{-}SNAP,23}$.

## 3.3 Liposome formation

In this section, we describe how we set up our model of the NK cell ADCC synapse using a SLB model system. To form the required SLB, we first produced very small liposomes, which facilitates the formation of a bilayer on a glass support.

1. Using glass Hamilton syringes, mix 1-palmitoyl-2-oleoyl-glycero-3-phosphocholine (POPC) and 1,2-dipalmitoyl-sn-glycero-3-[(N-(5-amino-1-carboxypentyl)iminodiacetic acid)succinyl] (DGS-NTA(Ni)) dissolved in chloroform at a 25:1 molar ratio in a glass tube. For a 20 mg preparation, mix 18.8 mg POPC and 1.2 mg DGS-NTA(Ni).
2. Cover the tube with parafilm, poke small holes with a needle, and dry lipid mixture under a vacuum filled with Drierite overnight at room temperature to remove all chloroform.
3. Add 1 mL PBS to the dried lipid film. Cover the tube with parafilm and shake at 37°C for 2 h.
4. Sonicate for 30 s in a water bath sonicator. Pipette up and down 2-3 times to fully resuspend the mixture.
5. Assemble Avanti Mini Extruder with a 0.8 μm filter between the O-rings and 2 Whatman filter papers on either side. Load lipid mixture into a Hamilton syringe and insert into the Mini Extruder. Insert an empty Hamilton syringe into the other side.

6. Press the lipid mixture through the filter 14 times at room temperature.
7. Repeat the above extrusion procedure using 0.4, 0.2, and 0.1 μm filters.
8. Store the 20 mg/mL, 100 nm liposomes in a glass vial at 4°C.

## 3.4 SLB preparation

In this section, we outline how supported lipid bilayers are generated and validated. In the model system described here, we include both HER2 and ICAM-1.

### 3.4.1 Generation of SLBs containing HER2 and ICAM-1

1. To clean glass coverslips, place coverslips in a glass staining chamber filled with acetone. Place the chamber inside a water bath sonicator and sonicate for 5 min. Repeat but replace acetone with 100 % ethanol. Repeat again but with MilliQ water. Between each step, dry coverslips with nitrogen gas. (*see* **Note 9**)
2. Further clean nitrogen dried coverslips with oxygen plasma with a power of 20 W and process pressure of 1.6 torr for 15 min (Fig. 1A). Use plasma cleaned coverslips within 30 min of cleaning.
3. Assemble the coverslip with the Ibidi sticky slide by removing the backing and placing the sticky slide directly on top of the glass coverslip, aligning the edges. Once assembled, carefully but firmly press the slide and coverslip together to ensure the chambers are fully sealed and to remove bubbles (Fig. 1B).
4. Add 50 μL of 4 mg/mL liposome suspension to each desired channel and incubate at room temperature for 20 min (Fig. 1C).
5. Wash each channel 10 times with PBS. (*see* **Note 10**)
6. Add 100 μM $NiCl_2$ containing 1 % (w/v) BSA for 20 min, then wash each channel with PBS 3 times (Fig. 1D).
7. Add His-tagged HER2 at 10 μg/mL and His-tagged ICAM-1 at 1 μg/mL (each in PBS) to each chamber and incubate at 37 °C for 60 min. After incubation wash the channel 3 time with PBS (Fig. 1E).

### 3.4.2 Confirmation of bilayer fluidity by fluorescence recovery after photobleaching (FRAP)

1. Add fluorescently labeled anti-HER2 antibody to each chamber at 10 μg/mL and incubate at room temperature for 30 min.
2. Wash each channel 3 times with PBS before moving sample to the microscope for imaging.

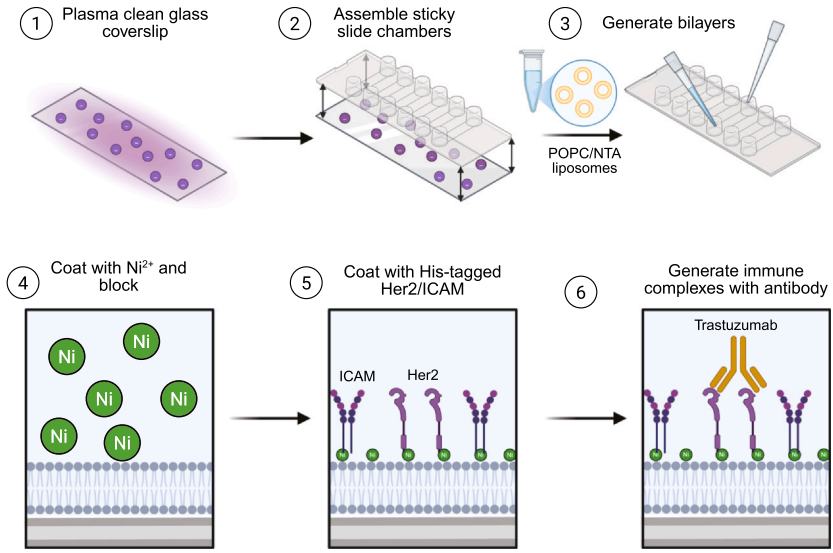


**Fig. 1 Assembly of chamber slides and supported lipid bilayers for generating immune synapses.** In this figure we outline the process of generating supported lipid bilayers (SLB) on glass to study NK cell antibody dependent cellular cytotoxicity (ADCC). 1) Clean #1.5 coverslips (the size of a standard glass microscopy slide) are plasma cleaned to produce a charge on the glass that promotes liposome assembly into bilayers. 2) Sticky slides (Ibidi) are assembled with the glass coverslip to create chambers that can each support a different experimental condition. 3) Small liposomes composed of POPC and NTA head groups are added to chambers, forming the bilayer. 4) Nickel is added to capture His-tagged antigens. 5) Antigens containing C-terminal His-tags are added in appropriate molar ratios. 6) Immune complexes are assembled on the bilayer using antibodies to target antigens (HER2), creating the final, artificial antigen presenting surface. *Created in BioRender. Murin, C. (2025) https://BioRender.com/1g9hrxp.*

3. On a confocal microscope, equipped with a 63 x/1.20 NA C-Apochromat water objective, apply immersion oil to the surface of the objective lens and then place the slide on the microscope stage. (*see* **Note 11**)
4. For FRAP studies, the following condition were used: excitation at 488 nm (7 % acousto-optic tunable filter (AOTF) transmission of a 35 mW Ar laser) with 493-630 nm emission detection window, 63x/1.2 NA C-Apochromat water objective, 0.77 μs pixel dwell time, 800 V gain, 0 offset, and 0.099 $\mu m^2$ pixel size.
5. Apply Perfect Focus with Zen and select the z-plane containing the maximum fluorescence intensity, which represents the surface of the bilayer. Lock this focus in place.

6. Select a small region of approximately 5 × 5 μm for photobleaching. After two scans, select a region of interest (ROI) of ~25 $\mu m^2$ and photobleach it (100 % power, 10 μs pixel dwell time, for a single scan). Record subsequent fluorescence recovery every 30 s for an additional 27 frames. FRAP analysis was performed in Zen software 2.3 SP1 FP3 (Black).

## 3.5 Synapse formation

In this section, we describe how a model NK cell IS is generated to investigate the spatial distribution of CD16a during ADCC.

1. Using coverslips prepared in *3.4.1*, add Trastuzumab at 10 μg/mL (in PBS) and incubate at room temperature for 30 min. Then wash each channel 3 times with PBS (Fig. 1F).
2. During incubation, count NK-92$^{CD16a\text{-}SNAP}$ cells and remove approximately 1 × $10^6$ cells from the flask.
3. Centrifuge cells at 100 × g for 5 min then resuspend cells in pre-warmed, serum-free RPMI.
4. After chambers are washed with PBS, add 100 μL of cell suspension to each chamber and incubate slide at 37 °C and 5 % $CO_2$ for 5 min.
5. Remove medium and wash excess cells from each chamber by gently washing with PBS 3 times. Then add pre-warmed 4 % (w/v) PFA in PBS to each chamber and incubate at room temperature for 15 min.
6. Subsequently remove excess PFA and directly add 0.4 % (v/v) Triton-X100 in PBS for 3 min to each chamber.
7. Then remove excess buffer and add 4 % (w/v) PFA in PBS solution again for 15 min.
8. After the second fixation step, remove excess buffer and wash with PBS, then replace buffer with 50 mM $NH_4Cl$ in PBS for 5 min.
9. Remove excess buffer and wash 3 times with PBS.

## 3.6 Sample labeling for MINFLUX imaging

After preparing the model IS, the sample is labeled for subsequent imaging. We used commercially available AF647-SNAP as the fluorescent label because AF647 demonstrates the necessary photophysical characteristics necessary for MINFLUX localization.

1. After synapse formation, block the sample with Image-iT for 30 min, then wash sample 3 times with PBS.
2. Label samples with 2 μM Alexa Fluor 647 SNAP ligand in 0.5 % (w/v) BSA with fresh 1 mM DTT in PBS for 50 min in the dark. (*see* **Note 12**)

3. Remove labeling solution and wash channels 3 times with PBS. After the third wash, add more PBS and incubate at room temperature for 30 min. Replace with fresh PBS and store overnight at 4 °C.
4. *Optional*: A stain for F-actin can be added to aid in locating cells and focusing the plane of the synapse. To do this, add Flash Phalloidin™ Green 488 to the PBS for overnight storage at 1:100 or 1:200. If staining for F-actin overnight, before imaging the next day, the sample must be washed 3 times with PBS before proceeding to the sample mounting step *3.7*.

## 3.7 Sample mounting for MINFLUX imaging

Critical to MINFLUX data acquisition is maintaining sample stabilization and preparing the buffer conditions for necessary fluorophore photoswitching. Here we describe the proper sample mounting protocol to support robust data acquisition during MINFLUX.

1. Remove PBS from samples that have been stored overnight. Reminder: if phalloidin staining was used, first wash samples 3 times with PBS. Gently rock the bottle of gold nanoparticles up and down to resuspend the gold, then add 100 μL of undiluted suspension to each chamber and allow to incubate at room temperature for about 5 min.
2. Wash samples 3–4 times to remove unattached gold nanoparticles. Additional washing can be performed if necessary to remove additional unstable nanoparticles (*see* **Note 13**).
3. Wash once with 100 μL of freshly prepared GLOX buffer then replace with fresh GLOX buffer. Then use a small piece of parafilm to tightly cover the end of the chamber to reduce exposure to the atmosphere (*see* **Note 14**).
4. Add immersion oil to the surface of the 100X objective lens then place the sample slide on the MINFLUX stage and clamp the slide securely in place with the coverslip facing the objective lens to proceed with image acquisition.

## 3.8 MINFLUX data acquisition

With the sample prepared, MINFLUX data can now be acquired by first identifying a region of interest (also known as a "ROI"), then initiating stabilization, and finally establishing single molecule photoswitching through laser-based fluorophore quenching and activation.

1. Open Imspector software. Important Live Dialogue menus used in this experiment are 'Minflux Data Panel', 'MINFLUX Acquisition', 'Stabilization', 'Channels', and 'Scan Range'. (*see* **Note 15**)

2. Using the oculars of the microscope, identify NK cells in brightfield mode, identify NK cells and find focus near the bottom face of the cell near the coverslip.
3. Switch the microscope to confocal mode with excitation at 640 nm with 650-720 nm emission detection window, 10 μs pixel dwell time, 180 nm pixel size, and 80 × 80 μm field of view to identify a desired cell and further refine focus.
4. Select a cell of interest with fluorescence intensity over background. The cell should be in a field that concurrently contains ~10 stable gold beads observable in the 'Stabilization' live dialog while the cell is located near the center of the field of view (Fig. 2A).
5. Adjust focus was so that the cell membrane closest to the coverslip is in view. This can be achieved using stained actin with the 488 laser primarily using the dial on the microscope control panel.
6. Select an area that includes the entire cell and copy this into another confocal overview window with excitation at 640 nm and emission detection at 650-720 nm, a 10 μs pixel dwell time, and an 80 nm pixel size (Fig. 2B). If necessary, further refine focus using the software-based focus option (Live Dialogue 'Scan Range') by adjusting the z-position by 100 nm or less before acquiring another confocal scan.
7. Initialize the stabilization system to compensate for potential sample drift over time following Abberior's instructions. The 'Stabilization' live dialog shows the camera stream of the gold nanoparticle reflection signal when the 'Ready' checkbox is activated. Choose a sample region for which ≥ 10 stably immobilized gold nanoparticles appear in the camera stream and avoid regions for which the camera stream shows less particles and/or flickering signal, indicating loosely immobilized particles.
8. Start the stabilization process by clicking 'Reference'. If needed, adapt masks defining regions to be included (green)/excluded (orange) from the reference process via the 'Include good areas'/'Exclude bad areas' input under the 'Advanced (show camera stream)' button and click 'Reference' again.
9. Lock the sample position, i.e. start active stabilizing of the sample in the referenced position by clicking the 'Lock' button. The msd in x- and y- should be <1 nm and z- <3 nm.
10. From the desired cell, select a ROI of approximately 3 × 3 μm to be used as the ROI for MINFLUX data collection and copy this into

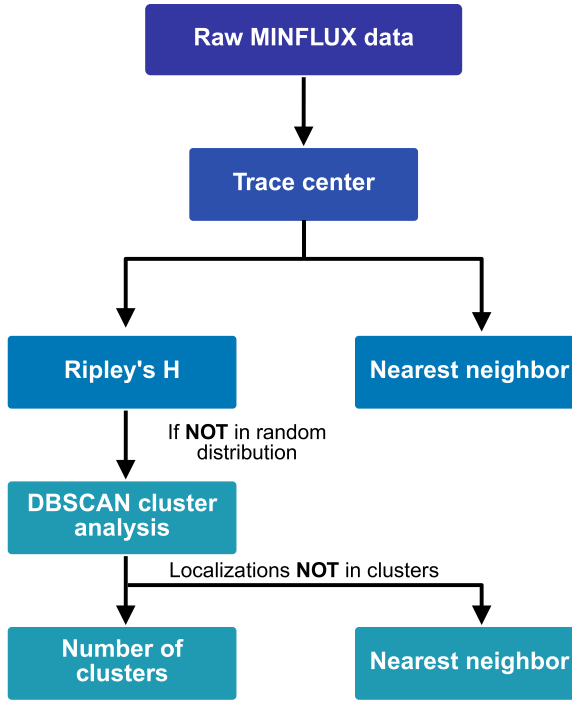


**Fig. 2 Data analysis workflow for MINFLUX nanoscopy collections**. Critical for obtaining biological insights from MINFLUX data is quantification of characteristics of the molecular localizations. The flow chart describes the data analysis pipeline used to analyze MINFLUX data. Raw MINFLUX data was first filtered, and the center of clusters identified provide the likely fluorophore localization. Fluorophore localizations were used to determine nearest neighbor distance. A second set of analysis of fluorophore localization was then used to determine if the data is clustered using Ripley's H. If the data was clustered, then clusters were identified using DBSCAN. The identified clusters were then counted. Secondary analysis was performed on localizations not in clusters, and pairs of localizations identified. Then the nearest neighbor distance between isolated pairs performed. *Created in BioRender. Murin, C. (2025)* https://BioRender.com/ptath8y.

another confocal overview window with excitation at 640 nm and emission detection at 650–720 nm, a 10 μs pixel dwell time, and a 20 nm pixel size (Fig. 2C).

**11.** Expand this region by ~1 μm in both x- and y- using the 'Scan Range' Live dialogue window before acquiring a confocal scan.

**12.** Scan this region repeatedly in confocal mode for approximately 10 frames, which pushes most of the fluorophores into a long-lived dark state (off-state) to reach the 'single molecule condition' (i.e. at most,

one fluorophore susceptible to 640 nm excitation "on-state" per MINFLUX probing area). The number of frames required to achieve this state will depend on the AOTF setting of the laser, amongst other factors listed in **Note 15** and **Note 16**.

13. Select the initial $3 \times 3$ μm ROI and then set as "MFX ROI".
14. Select the 2D MINFLUX sequence file in the "MINFLUX Acquisition" live dialogue box.
15. Click "MFX" to initiate localization measurement.
16. During the initial few minutes of measurement, the effective frequency at offset (efo) values may significantly fluctuate to >100 kHz. In MINFLUX, efo values are a measurement of emission frequency that reflects the number of photos collected from a fluorophore that is offset from the center of the doughnut excitation pattern. Efo values are a good way to monitor localization precision during your experiment. We find that values greater than 50 kHz provided an average localization precision of 2.5 nanometers. Once efo values are settled to <50 kHz and the number of recorded traces becomes sparse, use the 405 nm laser to increase the number of recorded traces.
17. Increase the power of the 405 nm laser slowly throughout the course of the experiment to maintain acquisition of localizations.
18. Monitor MINFLUX data quality through visualization of histograms of efo and center frequency ratio (cfr) using Paraview launched from inside the Imspector control software. The cfr is the ratio of emission frequency in the center of the doughnut excitation beam over the mean emission frequency across all the outer positions in the beam and can be used as an additional parameter of localization quality. Some studies have used cutoffs of 0.5 or better to gather only the most reliable localizations. These values should be monitored in real time to help determine if quality is significantly waning over the course of data collection (i.e. higher values closer to 1 could indicate poor data quality) (Schmidt et al., 2021).
19. Stop acquisition when appropriate (*see* **Note 16**) and save the measurement as a.msr file, and under the "MINFLUX Data Panel" live dialog in the "Export Data" section, specify the file path and select "as npy" to also export the data to a.npy file.

## 3.9 MINFLUX data processing

After MINFLUX data is acquired, careful analysis is important to extract meaningful biological insight. Here we established an analysis pipeline

that describes localization distribution as a whole, then further quantifies clustering and inter-fluorophore distances.

1. MINFLUX data was analyzed using custom scripts in either python or R, which can be found at https://github.com/pross1193/CD16-MINFLUX. Details on how to install and run these scrips can be found on the associated README.md file. A general outline of the data analysis will be described below (Fig. 3)
2. Before running the python script, input the MINFLUX data filtering criteria into the top of the script in the 'Set cluster variables' section. The input data required include:
   - min and max effective frequencies in offset (efo, background-corrected emission rates in Hz), to be set such that simultaneous emission events of more than a single molecule are excluded (*see* **Note 17**)
   - min and max time in which the trace (an attempted to localize a fluorophore) was acquired
   - max center frequency ratio (cfr, contrast between signals detected during center exposure and offset exposures of target-coordinate pattern), with cfr $< < 1$ indicating great contrast and cfr $= 1$ no contrast, to exclude low quality, i.e. poor contrast, localizations (*see* **Note 18**)

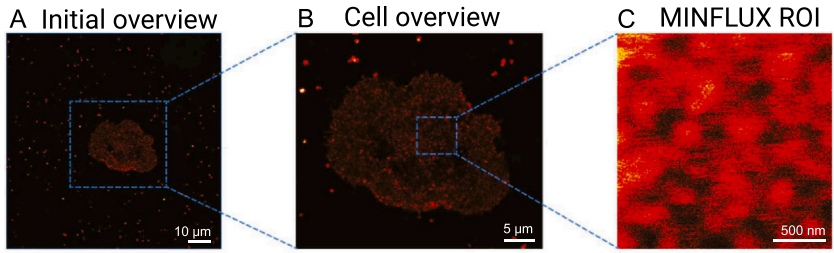


**Fig. 3 MINFLUX ROI selection**. To begin MINFLUX data acquisition, a region of interest must first be identified. The size of the ROI must be balanced with the desired throughput, as larger regions will take longer to scan. For NK synapse imaging, we typically select a ROI that is 3 $\mu m^2$, which provides several thousand localizations in a 1–3-hour session. A) A cell with fluorescence over background is first selected. B) The selected cell is copied into a new window to provide a cell overview. C) A sub-region of 3 µm x 3 µm is selected as the ROI for MINFLUX data collection. All data were collected in confocal mode on an Abberior MINFLUX and colored using the Fire lookup table 650–720 nm. *Created in BioRender. Murin, C. (2025) https://BioRender.com/vui6k6z.*

- minimum number of localizations for a valid trace (we rejected traces with fewer than 3 localizations)
- DBSCAN search radius for identification of a trace centers
- DBSCAN minimum number of localizations for identification of a trace center
- The directories used to save the output csv files

3. Input the filename and directories for data output.
4. Click 'Run' to run the python script. A dialogue box will pop up to select the.npy file exported from Imspector that includes the MINFLUX data.
5. While the script is running, the localization and trace statistics are extracted and placed into an array. The script then filters the data to remove low-quality and invalid traces and localizations based on the user input criteria. A scatter plot of the filtered data and trace centers is then generated for user validation.
6. The script next creates a histogram with the cluster localization precision of the trace centers.
7. The next function performs a nearest neighbor analysis to determine the distance between a trace center and the next closest trace center. Then the script saves both the trace center coordinates and nearest neighbor distances into a.csv file in the user defined directory.
8. Lastly, the script performs a Ripley H analysis (Ripley, 1977) to describe the degree of clustering of the trace centers and the output can be saved as a.csv file.
9. Next, run the R script to determine the clustering characteristics of the trace centers. Before running the R script, input the directory for the.csv file of the trace center coordinates generated by the python script.
10. The R script then creates a list of the trace centers and performs a DBSCAN cluster analysis (Ester et al., 1996; Pike et al., 2020). Importantly, input the analysis criteria for DBSCAN, including search radius and number of localizations per cluster. The value for the search radius and number of localizations per cluster was informed from the results published by the Owen lab (Bláha et al., 2022).
11. The script then creates a new data frame that includes the statistics of the clustered data that is saved as a.csv file. The script also generates a rendering of the trace centers colored by cluster for user visualization (Fig. 4A-B).

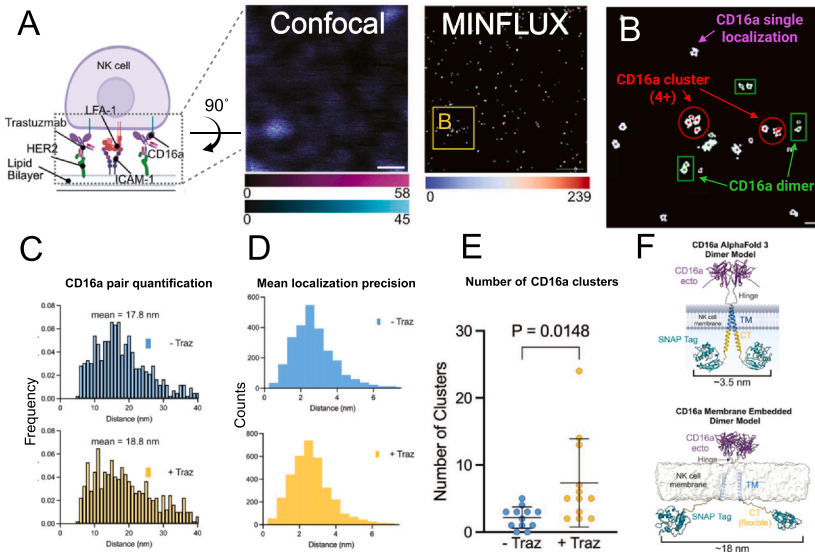


**Fig. 4 Example MINFLUX data from an NK cell ADCC immune synapse**. Here we provide an example MINFLUX data set acquired to study NK cell ADCC. A) The far-left cartoon shows a representation of the experimental setup described in sections 3.4–3.5. A lipid bilayer is assembled that displays Her2 and ICAM-1, which is then coated with Trastuzumab. Engineered NK-92/CD16a cells are added to generate a synapse. A ROI is selected within the resultant immune synapse (see Fig. 3) and imaged in confocal mode (middle, 650–685 nm in magenta and 685–720 nm in cyan). MINFLUX data is then collected on this ROI (far right, colored by DBSCAN cluster identity). B) The zoomed in region shows localization clouds, which are used to identify trace centers. Cluster analysis identified single localizations (purple), pairs (green, 2 localizations within a 40 nm radius), and clusters (red, 4 or more localizations within a 40 nm radius). Scale bars in confocal and MINFLUX images are 500 nm, and 50 nm in the zoomed in regions. C) Distances of pairs of localizations were quantified before ADCC activation (-Traz, blue) and after activation with Trastuzumab (+Traz, yellow). D) Localization precision for each coordinate determined by MINFLUX is plotted for pre- (-Traz, blue) and post-activation via ADCC (+Traz, yellow). Localization precision is determined as a mean of many localizations for the same position, which estimates the degree of uncertainty in its position. E) Cluster analysis using MINFLUX coordinates determined that clusters of 4 or more fluorophores within in 40 nm increases during NK cell ADCC activation (n = 12 cells). F) Molecular dynamics modeling and AlphaFold3 were used to determine potential structures of CD16a dimers, indicating that dimers were physiologically possible and that SNAP tag flexibility could account for the range of dimer distances we calculated in our study. *Created in BioRender. Murin, C. (2025)* https://BioRender.com/hnhqgzx.

## 4. Limitations

The protocol provided here has been optimized to study NK cell mediated ADCC with MINFLUX nanoscopy. Though we have applied this technique and acquired novel biological findings, critical limitations persist. Specifically, we are using NK-92 cell lines that do not normally express CD16a and therefore we needed to engineer an NK-92$^{CD16\text{-}SNAP}$ cell line. Future studies will attempt to use donor-derived NK cells and tag-free systems to maximize the biological relevance of our findings. Additionally, previous studies have demonstrated imperfect efficiency of SNAP-tag labeling as well as limitations in the ability to localize every fluorophore with MINFLUX nanoscopy. Thus, this prevents our ability to quantitatively localize every CD16a protein. Together, these limitations are being addressed through developing techniques in both chemical labeling and quantitative strategies to provide further biological insights (such as DNA-PAINT combined with MINFLUX) (Jungmann et al., 2014; Ostersehlt et al., 2022; Strauss & Jungmann, 2020).

## 5. Concluding remarks

The protocol presented here provides a method to investigate the NK cell immune synapse during ADCC. It provides a methodology to simulate CD16a engagement with immune complexes on a modeled target cell surface and then investigate receptor distribution at single molecule precision. The protocol requires the generation of a supported lipid bilayer system to model a target cell membrane that contains antibody opsonized antigen and ligands that assist in cell adhesion. We also describe how to generate NK-92 cells with genetically introduced receptors that include an endogenous fluorescent tag to facilitate MINFLUX imaging experiments with high precision, including confocal microscopy and MINFLUX nanoscopy. With this protocol, we have observed the presence of pairs of localizations ~18 nm apart (Fig. 4A-D) and detected increases in CD16a clusters of 4 or more single molecules within 40 nm upon activation (Fig. 4E). Combined with computational modeling, this suggests the possibility that CD16a forms homodimers on the NK cell membrane (Fig. 4F) (Ross et al., 2025). Notably, this type of direct observation would not have been possible without the level of spatial precision provided by MINFLUX nanoscopy. This protocol can easily be adapted to investigate

the function and effect of different antigens and antibodies on NK cell ADCC function and to other imaging modalities, including STED and other single molecule localization microscopy techniques. Furthermore, the application of MINFLUX nanoscopy using protocols like those reported here could be utilized to investigate the nanoscale distribution of other immune receptors in NK cell, T cell, and B cells during similar cytolytic processes, maturation, or expansion (for example, B-cell receptor selection/expansion). Combined with structural biology and computational modeling, these findings could unlock enhanced understanding of immune functions and provide novel therapeutic opportunities.

## 6. Notes

1. When cells are growing well, they will form small clumps. Before passaging cells, these clumps can be broken up by gently swirling the T flask or by gently pipetting up and down with a serological pipette. Media should also turn from red to orange.
2. If cells are ever thinned too far, their growth may slow or cease. They can be recovered by resuspending the cells in a smaller volume of fresh media in an appropriately sized cell culture vessel (for example, from a T-25 in 10 mL of media to a 6-well plate in 2 mL of media).
3. NK-92 cells can be scaled up to a T-75 during passaging. Use 25 mL of media with fresh IL-2 and stand the flask vertically. When growing robustly, the NK-92 cells can be split 1:5 without counting.
4. Before attempting to generate NK-92 cell lines, parental NK-92 cells should be passaged at least 3 times after recovery from liquid nitrogen and should be expanding when placed in fresh medium.
5. Plasmid concentration may need to be optimized to improve transfection efficiency. In our hands, a 3:1 (gene:transposon) ratio has provided acceptable transfection efficiency across different constructs.
6. When transferring cells to the cuvette, try to eliminate the formation of bubbles which can affect transduction efficiency and cell viability.
7. The time required between transfection and sorting can vary depending on transfection efficiency and how well cells recover. Under some circumstances, more time is need before cell sorting.
8. Cells were sorted using anti-CD16a antibody (3G8) labeled with AF647 at a dilution of 1:100 in PBS with 1 % FBS.

9. Cleaned coverslips can be stored under ethanol for up to a 1 week before use. Use nitrile gloves to handle coverslips. Coverslips can be placed on a Kim wipe between cleaning steps.
10. During all washing steps, make sure to not add bubbles to the channel and avoid allowing the channels to go dry. We recommend adding 200 μL of PBS to one side of the chamber and removing 100 μL from the opposite side for each wash.
11. Other objectives could also be used to perform these experiments.
12. This was usually performed by wrapping the slide with aluminum foil or placing the slide in a dish covered with aluminum foil.
13. Several gold particles stably attached to the coverslip in the same field of view of cells is crucial to the success of MINFLUX. Optimization of this step may be necessary to ensure robust data collection downstream.
14. GLOX buffer was prepared fresh each day by mixing: 50 mM Tris-HCl, 10 mM NaCl, 10 % (w/v) glucose, 10 mM cysteamine, 40 μg/mL bovine-liver catalase and 100 μg/mL glucose oxidase from *Aspergillus niger*, type VII, pH 8.0. We found that 10 mM of MEA generally worked to provide the necessary photoswitching properties for our samples. In some circumstances further optimization of MEA concentration may be required.
15. It should be noted that the details provided in the 'MINFLUX data acquisition section' are specific to the sample analyzed here (i.e. NK-92 cell immune synapses on SLBs) and that anyone wishing to replicate these studies will need to make adjustments for their samples depending upon several potential variables (e.g. reporter fluor used, cell type, micro-environment, quality of GLOX buffer components, MINFLUX laser power, etc.). These acquisition settings are meant to be an outline and starting point for other studies.
16. Data acquisition times depend on several factors, including primarily the number of fluorophores present in respective ROI, performance of photoswitching, and the type of data needed. We generally collected data on each ROI for approximately 3 h to be consistent. Some samples could have been observed for longer, though generally localization detection slowed down significantly after 3 h.
17. To determine max efo, plot a histogram of the efo values and select the value at the right side of the first distribution while avoiding higher values occurring from multiple fluorophores (i.e. the second peak). For our datasets, a threshold of 50 kHz was set for the efo filter.

18. To determine max cfr, plot a histogram of the cfr values and select a value <1 to include only valid localizations. The distribution should not commonly exceed about 0.95, which is what was used in our datasets.

## Acknowledgments

All confocal and MINFLUX microscopy data were collected at the Scripps Research Core Microscopy Facility, and we would like to thank Kathryn Spencer for her assistance. All cell sorting was performed at the Scripps Research Core Flow Cytometry Facility. We would like to thank Dr. Otto Wirth, Dr. Clara Gürth and Abberior Instruments for assistance with MINFLUX data acquisition, instrument and software troubleshooting, and data analysis. We would also like to thank Dr. Emily Mace for helpful discussions on experimental setup, and Dr. Dylan Owen for discussion on MINFLUX data analysis.

## Declaration of interests

JM is an employee of the company Abberior Instruments America, which commercializes super-resolution microscopy systems, including MINFLUX. The other authors declare no conflict of interest.

## References

Ambrose, A. R., Hazime, K. S., Worboys, J. D., Niembro-Vivanco, O., & Davis, D. M. (2020). Synaptic secretion from human natural killer cells is diverse and includes supramolecular attack particles. *Proceedings of the National Academy of Sciences of the United States of America, 117*, 23717–23720.

Balzarotti, F., et al. (2017). Nanometer resolution imaging and tracking of fluorescent molecules with minimal photon fluxes. *Science (New York, N. Y.), 355*, 606–612.

Bláha, J., et al. (2022). Structure of the human NK cell NKR-P1:LLT1 receptor:ligand complex reveals clustering in the immune synapse. *Nature Communications, 13*, 5022.

Ester, M., Kriegel, H.-P., Sander, J., & Xu, X. (1996). A density-based algorithm for discovering clusters in large spatial databases with noise. *kdd, 226*, 231.

Gwosch, K. C., et al. (2020). MINFLUX nanoscopy delivers 3D multicolor nanometer resolution in cells. *Nature Methods, 17*, 217–224.

Hazime, K. S., et al. (2025). Nanoscale restructuring of the immune synapse with an engager enhances NK cell function. *Proceedings of the National Academy of Sciences of the United States of America, 122*, e2507336122.

Jungmann, R., et al. (2014). Multiplexed 3D cellular super-resolution imaging with DNA-PAINT and Exchange-PAINT. *Nature Methods, 11*, 313–318.

Klingemann, H., Boissel, L., & Toneguzzo, F. (2016). Natural killer cells for immunotherapy – advantages of the NK-92 cell line over blood NK cells. *Frontiers in Immunology, 7*, 91.

Lanier, L. L., Phillips, J. H., Hackett, J., Tutt, M., & Kumar, V. (1986). Natural killer cells: Definition of a cell type rather than a function. *Journal of Immunology, 137*, 2735–2739.

Lanier, L. L., Ruitenberg, J. J., & Phillips, J. H. (1988). Functional and biochemical analysis of CD16 antigen on natural killer cells and granulocytes. *Journal of Immunology, 141*, 3478–3485.

Mace, E. M., & Orange, J. S. (2013). New views of the human NK cell immunological synapse: Recent advances enabled by super- and high-resolution imaging techniques. *Frontiers in Immunology, 3*, 421.

Mace, E. M., & Orange, J. S. (2014). Lytic immune synapse function requires filamentous actin deconstruction by Coronin 1A. *Proceedings of the National Academy of Sciences of the United States of America, 111*, 6708–6713.

Mace, E. M., et al. (2012). NK cell lytic granules are highly motile at the immunological synapse and require F-Actin for post-degranulation persistence. *Journal of Immunology, 189*, 4870–4880.

Mace, E. M., et al. (2014). Cell biological steps and checkpoints in accessing NK cell cytotoxicity. *Immunology and Cell Biology, 92*, 245–255.

Mukherjee, M., Mace, E. M., Carisey, A. F., Ahmed, N., & Orange, J. S. (2017). Quantitative Imaging approaches to study the CAR immunological synapse. *Molecular Therapy, 25*, 1757–1768.

Orange, J. S. (2008). Formation and function of the lytic NK-cell immunological synapse. *Nature Reviews. Immunology, 8*, 713–725.

Ostersehlt, L. M., et al. (2022). DNA-PAINT MINFLUX nanoscopy. *Nature Methods, 19*, 1072–1075.

Pike, J. A., et al. (2020). Topological data analysis quantifies biological nano-structure from single molecule localization microscopy. *Bioinformatics (Oxford, England), 36*, 1614–1621.

Rak, G. D., Mace, E. M., Banerjee, P. P., Svitkina, T., & Orange, J. S. (2011). Natural killer cell lytic granule secretion occurs through a pervasive actin network at the immune synapse. *PLoS Biology, 9*, e1001151.

Ripley, B. D. (1977). Modelling spatial patterns. *The Journal of the Royal Statistical Society, Series B (Methodology), 39*, 172–192.

Ross, P., et al. (2025). CD16a pairs form the basal molecular subunit for the NK-cell ADCC lytic synapse. *Journal of Immunology*. https://doi.org/10.1093/jimmun/vkaf077.

Rossy, J., Pageon, S. V., Davis, D. M., & Gaus, K. (2013). Super-resolution microscopy of the immunological synapse. *Current Opinion in Immunology, 25*, 307–312.

Sajman, J., et al. (2021). Adhering interacting cells to two opposing coverslips allows super-resolution imaging of cell-cell interfaces. *Communications Biology, 4*, 439.

Schmidt, R., et al. (2021). MINFLUX nanometer-scale 3D imaging and microsecond-range tracking on a common fluorescence microscope. *Nature Communications, 12*, 1478.

Steblyanko, M., Anikeeva, N., Campbell, K. S., Keen, J. H., & Sykulev, Y. (2015). Integrins influence the size and dynamics of signaling microclusters in a Pyk2-dependent manner. *Journal of Biological Chemistry, 290*, 11833–11842.

Strauss, S., & Jungmann, R. (2020). Up to 100-fold speed-up and multiplexing in optimized DNA-PAINT. *Nature Methods, 17*, 789–791.

Zheng, P., Bertolet, G., Chen, Y., Huang, S., & Liu, D. (2015). Super-resolution imaging of the natural killer cell immunological synapse on a glass-supported planar lipid bilayer. *Journal of Visualized Experiments: Jove,* 52502. https://doi.org/10.3791/52502.